Jour. Korean Inst. Mining Geol.
Vol. 19, No. 3, p. 219-224, 1986

Analyses of Spectral IP Responses over 20-Degree Dipping Structure

Hee Joon Kim*

Abstract: Spectral induced polarization (IP) responses for 20-degree dipping body are obtained by both numerical and scale models. The IP responses for the dipping body vary not only with current frequencies but also with resistivity ratios between the body and the surrounding medium. If the ion concentration related to polarizable reaction is constant, the resistivity of polarizable body depends only on the current frequency. This implies that the IP responses to the resistivity ratio are qualitatively equivalent to those to the current frequency. The numerical results with wide-range resistivity ratios, therefore, can be used as standard curves for the interpretation of spectral IP data.

INTRODUCTION

The method of induced polarization (IP) is based on the frequency dependence of resistivity of rocks. In spectral IP (or multi-frequency IP), the apparent resistivity is measured in a wide-frequency band (e.g., 1/1024, ..., 1024 Hz). Thus the spectral IP can be regarded as a more refined form of the conventional IP. This type of survey becomes possible with the development of electronics.

On the basis of complex resistivity measurements, Pelton et al. (1978) showed that variations in the frequency spectra of resistivity arise mainly from mineral texture. They also showed that it is possible to recognize and to remove the effect of inductive electromagnetic (EM) coupling from the IP spectra by means of Cole-Cole relaxation models. In the conventional IP, the EM coupling was regarded as a kind of noise. In the spectral IP, however, the EM coupling can play an important role in detecting low-resistivity ore deposits (Wynn and Zonge, 1975) and man-made grounded structures (Nelson, 1977). The recognition and removement of EM coupling is usually carried out by using Cole-Cole plots of complex resistivity. But this procedure requires too much time and has little advantage in delineating the subsurface structure.

It this paper, spectral IP responses over a 20-degree dipping structure are obtained by the scale model experiment which has little EM coupling. Simple explanations for these results are conducted by means of sample measurments and numerical models. As a result it will be shown that the spectral IP responses are qualitatively equivalent to the IP responses varying with resistivity ratios between targets and host rocks. It will be also shown that the numerical results with the wide-range resistivity ratios can be used for standard curves in the spectral IP.

MODELS

To illustrate the effects of current frequency on the apparent resistivity response in the scale model experiment, a dipping model is selected in this study (Fig. 1). The polarizable body is a pyrite in Yanahara, Japan, and its size is $5\times 2\times 0.5$ units (dipole length, 2 cm in the scale model). The body is inclined 20 degrees against the X-Y plane ($Z=0$). The shallowest position of the body is 1 unit apart from the X-Y plane

* Department of Applied Geology, National Fisheries University of Pusan.

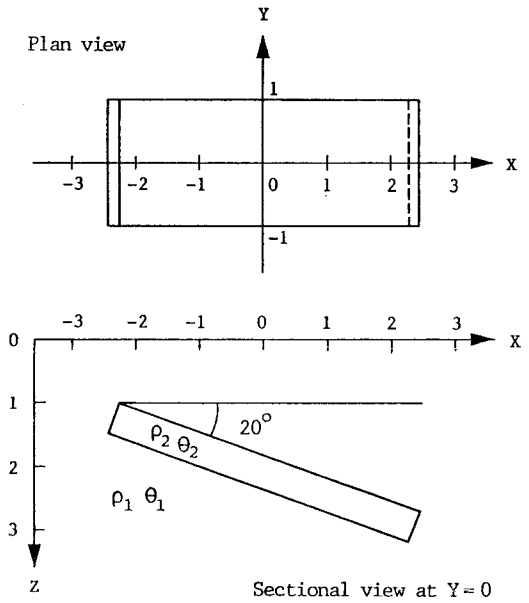

Fig. 1 Plan and sectional views of the 20-degree dipping body in scale model. The resistivity and phase of body are ρ_2 and θ_2, respectively, and those of surrounding medium are ρ_1 and θ_1, respectively. All dimensions are in units of dipole length.

and the center of the body is just below the origin. The resistivity of surrounding medium is kept in $\rho_1=12.5\ \Omega\cdot$m and its phase is $\theta_1=0$, i.e., non-polarizable. Apparent resistivities are measured with dipole-dipole array for four frequencies of current: 0.1, 0.3, 1 and 3 Hz. Details of the equipment of scale model experiment are shown in Noguchi et al. (1982).

Results of scale model experiment are compared with those of numerical model calculation. The numerical model is the same as Kim (1984). The numerical results, therefore, are obtained as complex apparent resistivities and shown as functions of the normalized apparent resistivity (ρ_a/ρ_1) and phase ($B_2=\theta_a/\theta_2$), where ρ_a and θ_a are the calculated amplitude and phase of complex apparent resistivity, respectively, and θ_2 is the assigned phase of body resistivity. All profile lines shown in this paper are perpendicular to the strike of dipping body ($Y=0$ in Fig. 1).

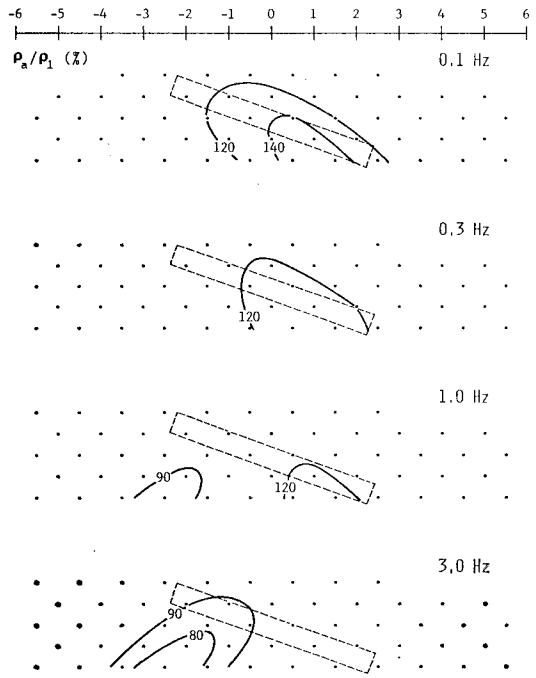

Fig. 2 Effect of current frequency (0.1, 0.3, 1 and 3 Hz) on apparent resistivity responses for the 20-degree dipping body in the scale model.

SCALE MODEL EXPERIMENT

Fig. 2 shows dipole-dipole apparent resistivity responses of the dipping body at four current frequencies: 0.1, 0.3, 1 and 3 Hz. In the case of 0.1 Hz, high-resistivity anomalies appear in the position nearly identical to the body. The high-resistivity anomaly in the body position decreases with an increase of current frequency, and it is lost in 3 Hz. The anomaly pattern in 0.3 Hz is almost the same as in 0.1 Hz. In the case of 3 Hz, only low-resistivity anomalies occur on the side opposite to the direction of dip. The low-resistivity anomaly becomes weak with a decrease of current frequency, and it is lost in 0.3 Hz. The result in 1 Hz has both low- and high-resistivity anomalies, and these magnitudes are relatively small. Note that the scale model experiment has little EM couplings mainly due

to short dipole length (2 cm). Also note that the resistivity of surrounding medium and the concentration of Fe^{2+} and Fe^{3+} associated with polarizable reactions are kept in constant in the experiment.

Noguchi (1979) showed that, by means of sample measurements of pyrite, the resistivity of polarizable body measured by fine currents depends on two factors: the ion concentration associated with polarizable reactions and the period of transmitting current. This implies that the polarizable body has no inherent resistivity in spectral IP. Since the ion concentration in the scale model experiment is constant, the body resistivity varies with the current frequency. In other words, the change of frequency is basically equivalent to that of resistivity ratio between the body and the surrounding medium.

Fig. 3 shows a relation between the resistance of pyrite and the current period in the sample measurement (Noguchi, 1979). From this figure we see that the sample resistance R is proportional to the root period of current T, i.e.,

$$R \propto \sqrt{T} = 1/\sqrt{f},$$

where f is the current frequency. This implies that in the scale model experiment the apparent resistivity of polarizable body and the resistivity ratio decrease with an increase of current frequency. Note that the geometric effect of the body should be considered in estimating body resistivity ρ_2 at a certain frequency.

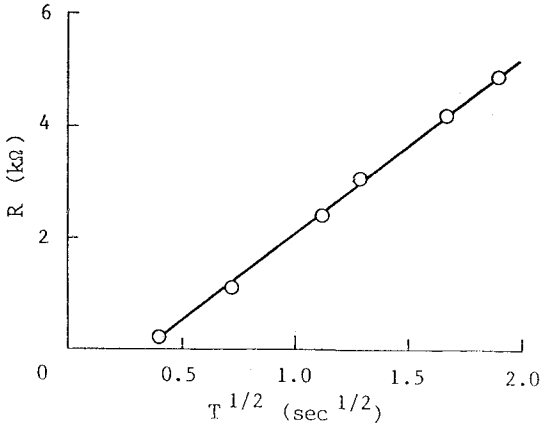

Fig. 3 Relation between the resistance (R) and the current period (T) obtained from the sample measurement (after Noguchi, 1979).

NUMERICAL CALCULATION

Fig. 4 compares apparent resistivity responses of the dipping body for four resistivity ratios: ρ_2/ρ_1=16, 4, 1/4 and 1/16. For the resistive bodies (ρ_2/ρ_1=16 and 4), high-resistivity anomalies appear at the position nearly identical to the body, while for the strongly conductive body (ρ_2/ρ_1=1/16), a low-resistivity anomaly inclines in the direction opposite to the body. For the weakly conductive body (ρ_2/ρ_1=1/4), on the other hand, relatively broad and low-amplitude anomaly appears around the body position, and anomaly pattern is nearly symmetrical in spite of asymmetrical body shape. From Figs. 2 and

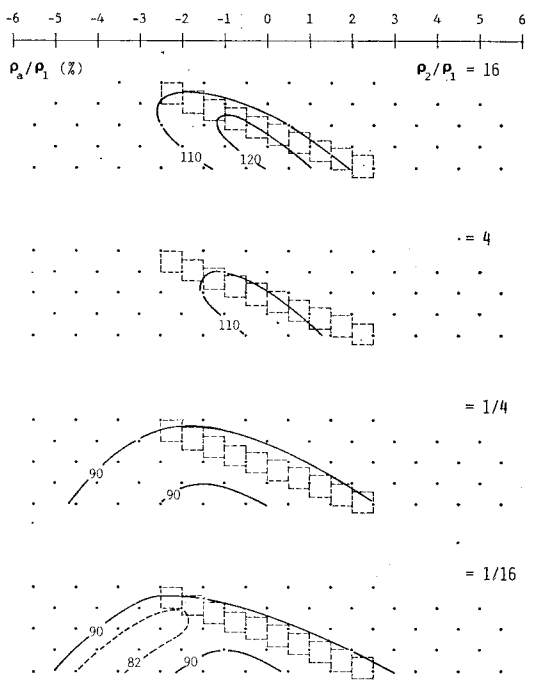

Fig. 4 Effect of resistivity ratio (ρ_2/ρ_1=16, 4, 1/4 and 1/16) on apparent resistivity responses for the 20-degree dipping body in the numerical model.

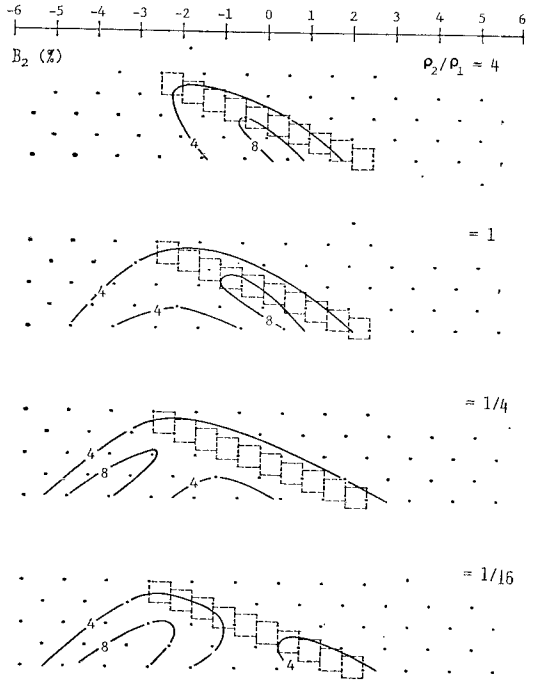

Fig. 5 Effect of resistivity ratio ($\rho_2/\rho_1=4, 1, 1/4$ and $1/16$) on B_2 responses for the 20-degree dipping body in the numerical model.

4, we see that the patterns of anomaly variation with current frequencies are similar to those with resistivity ratios.

Fig. 5 shows IP responses (B_2) of the dipping body for four resistivity ratios: $\rho_2/\rho_1=4$, 1, 1/4 and 1/16. For the resistive bodies ($\rho_2/\rho_1>1$), the largest B_2 anomalies appear at the position nearly identical to the body. For the conductive bodies ($\rho_2/\rho_1<1$), however, the largest B_2 anomalies incline in the direction opposite to the body. Note that B_2 anomalies can be defined even in $\rho_2/\rho_1=1$, but apparent resistivities are not so.

Fig. 6 shows relations between IP responses and resistivity ratios at points $C_{-6,-5}P_{-1,0}$ and $C_{-3,-2}P_{2,3}$, respectively. Details for the points are explained in Kim (1984). From this figure we see that B_2 curves vary with plotting points in the pseudo-section. The $C_{-6,-5}P_{-1,0}$ has a peak B_2 anomaly in the conductive region ($\rho_2/\rho_1\cong$

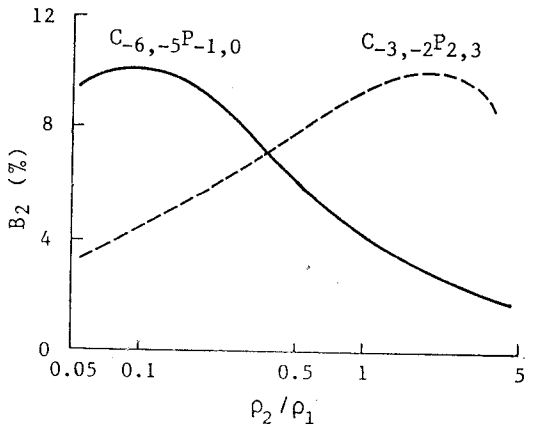

Fig. 6 B_2 curves at the points of $C_{-6,-5}P_{-1,0}$ and $C_{-3,-2}P_{2,3}$ for the 20-degree dipping body in the numerical model.

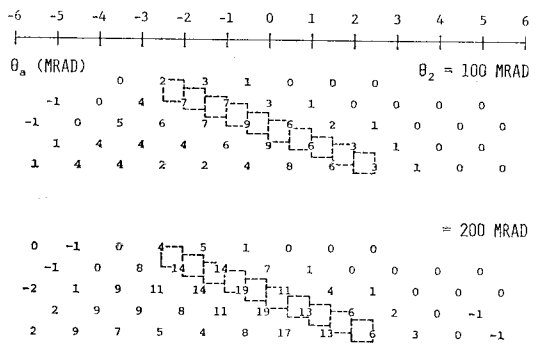

Fig. 7 Effect of intrinsic phase ($\theta_2=100$ and 200 mrad) on apparent phase responses for the 20-degree dipping body in the numerical model. The resistivity ratio is $\rho_2/\rho_1=1$.

0.1), while the $C_{-3,-2}P_{2,3}$ has a peak in the resistive region ($\rho_2/\rho_1\cong 2$).

Fig. 7 compares apparent phase responses of the dipping body for two intrinsic (assigned) phases: $\theta_2=100$ and 200 mrad. The body resistivity is the same as the background resistivity, i.e., $\rho_2/\rho_1=1$. From this figure we see that the apparent phase response in $\theta_2=200$ mrad is two times more than the value in $\theta_1=100$ mrad at the corresponding point. The anomaly pattern, therefore, does not change with the intrinsic phase of body. In the numerical model the B_2 is the ratio of the calculated apparent phase (θ_a) to the intrinsic phase of the body (θ_2). Thus the

result of Fig. 5 is equivalent to the apparent phase response for $\theta_2=100$ mrad.

DISCUSSION AND CONCLUSIONS

The frequency domain and the time domain are equivalent in a linear and causal system, and these domains are connected through the Fourier transform. The time domain is attractive because the whole transient can be recorded in a single measurment, so there are many divices in commercial use. Interpretation, however, is difficult in the time domain because Ohm's low must be transformed to convolution integral in the time domain. Hence one should transform the time-domain data to the frequency domain by the Fourier transform. But in practice, the information obtained from time-domain measurements cannot be transformed to the information of wide-band resistivities in the frequency domain (Soininen, 1984). It is advisable that the transformation from time domain to frequency domain is limitted in harmonics up to 9 or 11 orders for one frequency (Noguchi et al., 1982). In this study the transformation was not carried out because the scale model experiment involves little EM coupling and also because the information of intermediate frequency is not needed in determining the subsurface structure.

IP responses of both apparent resistivity and phase vary with the resistivity ratio (Figs. 4 and 5). Roughly speaking, the resistive dipping body has high-resistivity and large B_2 (or phase) anomalies in the same side of the body, while the conductive body has low-resistivity and large B_2 anomalies in the opposite side of the body. The resistivity ratio with peak B_2 anomaly also vary with plotting points in the pseudo-section (Fig. 6). From these results we see that the resistivity ratio is a very important factor in changing the position with large IP anomaly. When we interpret the field data, therefore, the resistivity ratio between targets and host rocks should be estimated first.

From Fig. 2 we see that the apparent resistivity patterns of the dipping body change dramatically with current frequency in the scale model experiment. Noguchi (1979) showed that, through the sample measurment of pyrite, if the ion concentration related to the polarizable reaction is constant, the resistivity of polarizable body is determined only by current periods (Fig. 3). This implies that if the background medium is non-polarizable, changing the resistivity ratio can be carried out by changing the current frequency (period) in the scale model experiment or in the field. The change of pattern in Fig. 2, therefore, is qualitatively equivalent to that in the numerical model of Fig. 4. The estimation of body resistivity (or resistivity ratio) has not been made in this study. Such estimation for a cubic body was made by Takeuchi et al. (1974).

From Figs. 5 and 7 we know that the IP pattern does not change with the intrinsic body phase (θ_2) but change only with the resistivity ratio (ρ_2/ρ_1). When we consider the equivalency between resistivity ratio and current frequency, therefore, the apparent resistivity and B_2 anomalies of Figs. 4 and 5 can be used for standard curves in data analysis of spectral IP. By using these standard curves, more accurate data analysis is expected for dipping structures. The key-point of the analysis is to trace the movement of large anomaly (or the change of anomaly pattern) with the change of current frequency or resitivity ratio.

ACKNOWLEDGEMENTS

I wish to thank to Dr. K. Noguchi, Waseda Univ., for his helpful comments on this work, and to Dr. Y.Q. Kang, Nat. Fish. Univ. Pusan, for his careful reading of the manuscript.

REFERENCES

Kim, H.J. (1983) Three-dimensional standard curves in induced polarization method. J. Korean Inst. Mining Geol., v. 16, No. 4, p. 269-276.

Kim, H.J. (1984) Analyses of dipole-dipole IP responses over dipping structures. J. Korean Inst. Mining Geol., v. 17, No. 1, p. 49-55.

Nelson, P.H. (1977) Induced-polarization effects from grounded structures. Geophysics, v. 42, No. 6, p. 1241-1253.

Noguchi, K. (1979) Study on the polarizable effect of ores in electrical prospecting. D. Eng. Thesis, Waseda Univ., 176 pp. (in Japanese)

Noguchi, K., Takeuchi, M., Kim, H.J. and Endo, G. (1982) Study on the systematization of the process from measurement to analysis in electrical prospecting. Butsuri-Tanko, v. 35, No. 2, p. 77-84. (in Japanese)

Pelton, W.H., Ward, S.H., Hallof, P.G., Sill, W.R. and Nelson, P.H. (1978) Mineral discrimination and removal of inductive coupling with multifrequency IP. Geophysics, v. 43, No. 3, p. 588-609.

Soininen, H. (1984) Inapplicability of pulse train time-domain mesurments to spectral induced polarization. Geophysics, v. 49, No. 6, p. 826-827.

Takeuchi, M., Noguchi, K. and Endo, G. (1974) Study on the three-dimensional modeling of strata in electrical prospecting: In the case of induced polarization method. Butsuri-Tanko, v. 27, No. 5, p. 189-200. (in Japanese)

Wynn, J.C. and Zonge, K.L. (1975) EM coupling, its intrinsic value, its removal and the cultural coupling problem. Geophysics, v. 40, No. 5, p. 831-850.

20도 경사구조에 대한 스펙트럴 IP응답의 해석

김 희 준

요약 : 20도 경사물체에 대한 스펙트럴 IP응답을 수치모델 및 축소모델로 구하였다. 이들 응답은 송신주파수 뿐만 아니라 물체와 주위의 비저항비에 따라서 변한다. 가령 분극반응에 관련된 이온 농도가 일정하다면 분극체의 비저항은 송신주파수에만 의존한다. 이는 비저항비가 IP응답에 미치는 효과는 송신주파수의 효과와 정성적으로 일치한다는 것을 뜻한다. 따라서 비저항비별로 구한 수치계산 결과는 스펙트럴 IP데이터 해석의 표준곡선으로 사용할 수 있다.